



ELSEVIER

Contents lists available at ScienceDirect

Ocean Engineering

journal homepage: www.elsevier.com/locate/oceaneng

Research paper

An autonomous surface vehicle for acoustic tracking, bathymetric and photogrammetric surveys

Pierre Gogendeau ^a, Sylvain Bonhommeau ^a, Hassen Fourati ^b, Mohan Julien ^a,
Matteo Contini ^a, Thomas Chevrier ^c, Anne Elise Nieblas ^c, Serge Bernard ^{d,*}

^a IFREMER DOI, Le Port, 97420, Réunion, France

^b Univ. Grenoble Alpes, CNRS, Inria, Grenoble INP, GIPSA-Lab, Grenoble, 38000, France

^c COOOL SAS, Saint-Leu, 97436, Réunion, France

^d LIRMM/CNRS University of Montpellier, Montpellier, 34000, France

ARTICLE INFO

Keywords:

Acoustic tracking
ASV
Bathymetry
Open-source
Photogrammetry

ABSTRACT

Autonomous Surface Vehicles (ASVs) are becoming increasingly affordable and versatile, integrating a wide range of sensors for applications ranging from oceanographics to marine wildlife monitoring. However, the high cost and limited adaptability of commercial ASVs remain major barriers for many research applications, particularly in ecology. To address these challenges, we developed a low-cost, open-source, and reproducible ASV designed for multi-modal surveys. The ASV enables autonomous acoustic tracking of marine animals equipped with acoustic tags, achieving a mean spatial accuracy of 1 m (standard deviation of 1.8 m) over 4.5 h of continuous monitoring. Additionally, the ASV efficiently performs bathymetric surveys that meet Class 1 hydrographic survey standards, and photogrammetric surveys with a mean horizontal accuracy of 0.51 m and a vertical accuracy of 0.66 m (CE90 and LE90 metrics, respectively). The cost of the ASV varies between about US\$2500 to US\$11,000, depending on sensor configurations, making it significantly more affordable than commercial alternatives. Field validations confirm the ASV's ability to deliver high-quality, reliable data, offering an accessible and adaptable solution for ecological and environmental monitoring.

1. Introduction

Most unmanned surface vehicles (USVs) and autonomous surface vehicles (ASVs) are highly expensive and developed primarily for military applications (Liu et al., 2016; Yan et al., 2010), the industrial operations (Hodges et al., 2023), or large-scale scientific research (Kimball et al., 2014; Campos et al., 2024). However, in recent years, several projects have emerged, proposing small, low-cost ASV/USV under \$ 5000, though these typically lack specialized sensors (Chaysri et al., 2024; Raber and Schill, 2019; Lambert et al., 2020). This increase in affordability has been driven by the increased availability of low-cost, open-source and reliable electronics and marine robotic parts, which have democratized ASV development and enhanced their accessibility to smaller-scale ventures. For example, the T200 thruster, a popular propulsion unit made by *Blue Robotics*, is now widely used by many hobbyists (Boogie Board Boat, 2022), scientists (Sotelo-Torres et al., 2023), and industrial projects. A similar evolution has taken place in software development. Both profession-

als and hobbyists contribute to the development of high-quality, user-friendly, well-documented, and open-source autopilots systems. For example, *Ardupilot* is now embedded in various vehicles such as drones, rovers, remotely operated vehicles (ROVs), boats, and ASVs (Zhao et al., 2020; Baldi et al., 2022; Wardoyo et al., 2022). Beyond navigation, *Ardupilot* provides data logging, analysis, and simulation capabilities. The open community linked to these projects fosters continuous innovation and rapid technological advancements, making low-cost ASVs more viable than ever for scientific and environmental applications (Fig. 1).

Building on these advancements in low-cost marine robotics, we developed an ASV designed to perform key scientific tasks in marine environments. In this paper, we present an ASV developed for three main missions:

- Autonomous acoustic tracking of a marine animal;
- Bathymetric surveys; and
- Photogrammetric surveys.

* Corresponding author.

E-mail addresses: pierre.gogendeau@gmail.com (P. Gogendeau), sylvain.bonhommeau@ifremer.fr (S. Bonhommeau), hassen.fourati@grenoble-inp.fr (H. Fourati), mohan.julien@ifremer.fr (M. Julien), Matteo.Contini@ifremer.fr (M. Contini), t.chevrier.coolresearch@gmail.com (T. Chevrier), cool.research@gmail.com (A.E. Nieblas), serge.bernard@cnrs.fr (S. Bernard).

<https://doi.org/10.1016/j.oceaneng.2025.121201>

Received 21 June 2024; Received in revised form 16 March 2025; Accepted 7 April 2025

Available online 28 April 2025

0029-8018/© 2025 The Authors. Published by Elsevier Ltd. This is an open access article under the CC BY license (<http://creativecommons.org/licenses/by/4.0/>).

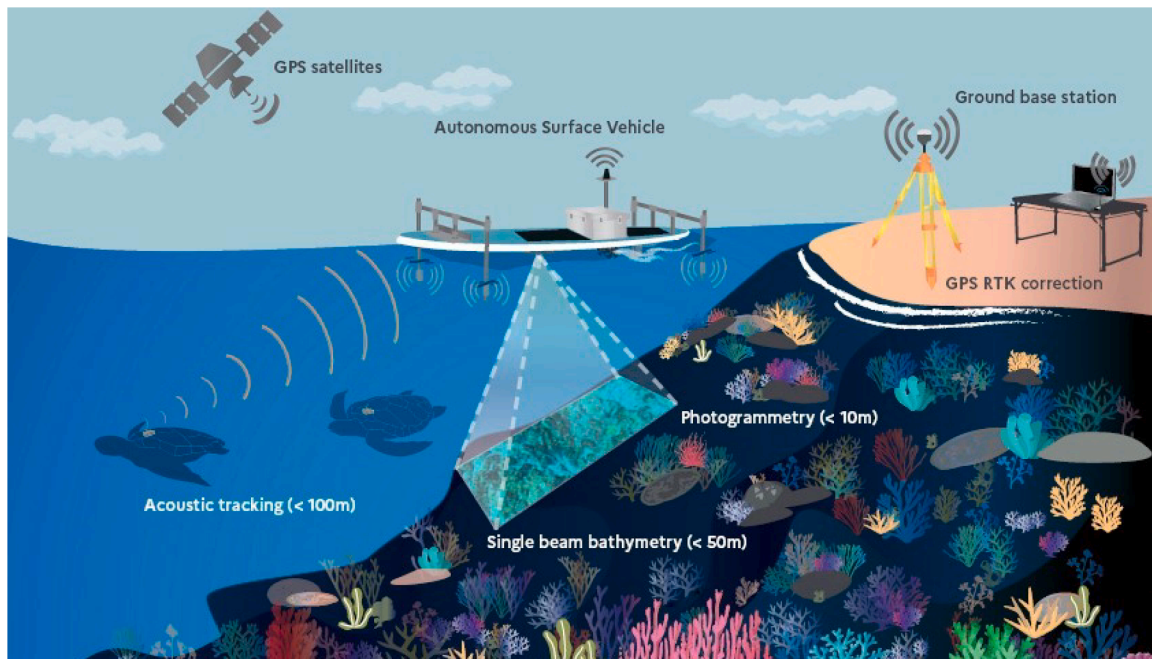


Fig. 1. Schematic of the functioning of the autonomous surface vehicle (ASV) and the data collected during an ASV survey: Autonomous acoustic tracking, single-beam bathymetric survey, and photogrammetric survey.

1.1. Autonomous acoustic tracking of a marine animal

Advances in biologging technology, which produces geolocated trajectories have enabled fine-scale tracking of marine animals, providing valuable insights into habitat use and behavior. Biologging refers to the deployment of autonomous devices on free-ranging animals to collect physical and biological information through different sensors (Iwata and Akamatsu, 2025). A common technique for geolocated trajectory estimation of marine animals is dead-reckoning, which integrates inertial data, sensor speed, and GPS positions to track movement over time (Gogendeau et al., 2022). Though effective, dead-reckoning requires tag recovery, high computing effort, and is subject to cumulative errors (Gunner et al., 2021).

Underwater fine-scale geolocated tracking is also possible with acoustic systems composed of transmitters and receivers. Some systems with anchored or buoy receivers need dense acoustic antenna arrays (Shiple et al. (2024) to use their geolocation algorithms. These systems are not adapted for marine species that travel several kilometers per day. Some other acoustic systems are more compact, like ultra-short baseline (USBL) and short baseline (SBL) acoustic systems. USBL and SBL systems calculate the range of an acoustic transponder based on the time of arrival or time of flight (TOF) of the signal. In addition, USBL uses a phase-differencing algorithm with the receiver baseline to obtain the bearing angle Liu et al. (2024). With the calculated relative position, both systems infer the geolocated position of the transponder by adding the global navigation satellite system (GNSS) position of the receiver system. USBL receiver systems are more compact and offer a better range and accuracy than SBL systems. For example, for Blue Print USBL,¹ the range is 1 km with 0.1 m accuracy compared to 100 m with 1 m accuracy of the Waterlinked UGPS G2 SBL.² USBL systems have successfully been installed on autonomous underwater vehicles (AUVs) Dodge et al. (2018) and Page et al. (2021) for animal tracking. For example, Dodge et al. (2018) were able to follow a turtle with their AUV for several hours with a USBL system. However, some drawbacks of the USBL sys-

tems include higher cost, larger transmitter size and reduced accuracy in shallow environments.

Given these considerations, we aimed to develop an accurate, fine-scale tracking systems for juvenile green turtles (*Chelonia mydas*) inhabiting the shallow reefs of Reunion Island in the western Indian Ocean. Green turtles play a crucial ecological role in maintaining healthy seagrass beds and coral reef ecosystems, yet their movement patterns in shallow coastal habitats remain poorly understood. Understanding their fine-scale movements is essential for assessing habitat use, identifying critical foraging areas, and informing conservation strategies Chambault et al. (2020). To balance accuracy and feasibility, we selected the SBL Waterlinked UGPS G2 system to estimate the underwater positions. To address the 100-m range constraint, we adapted the ASV navigation system to follow the acoustic transponder within this range.

1.2. Bathymetric survey

Bathymetry surveys using ASVs are generally performed by professionals, as they require high-cost sensors such as an echosounder and a differential GPS for sub-centimetric positioning. An echosounder measures depth by sending acoustic signals to the seafloor, which bounce back to the sounder, thus measuring the depth based on the travel time and velocity of the signal in water. These surveys are commonly used to map harbors and navigation channels. For the ecological purposes of this study, the bathymetric data can be compared with the animal's recorded depth to better understand its use of the water column during key behaviors such as resting or feeding Dodge et al. (2018).

As with other electronic systems, the cost of bathymetric sensors has decreased over time. For example, an ECT-400 echosounder³ was initially priced at US\$ 3700 in 2022 with the equivalent sensor, the S-500 by Cerulean,⁴ is available for US\$ 890 in 2025. Several projects emerged in the past few years integrating bathymetry sensors into ASVs (Hyun et al., 2023; Sotelo-Torres et al., 2023; Carlson et al., 2019), but these are not easily reproducible or do not fit our purposes. For instance,

¹ <https://www.blueprintsubsea.com/seatrac/seatrac-lightweight>

² <https://store.waterlinked.com/product/underwater-gps-g2/>

³ <https://www.echologger.com/products/single-frequency-echosounder-deep>

⁴ <https://ceruleansonar.com/products/sounder-s500>

the project by [Hyun et al. \(2023\)](#) is not open source. In addition, most studies do not specify the bathymetry accuracy, making it difficult to assess their compliance with standardized survey requirements. In our project, we aim to achieve the Order 1a bathymetry standard from the Hydrographic Surveys reference [Organization \(2020\)](#) and to discriminate small seabed features within at least a 5 m radius. Additionally, cost constraints also limits the feasibility of using multibeam echosounders which remain an impractical option, often priced in the tens of thousands of dollars.

1.3. Photogrammetric survey

Photogrammetry enables three-dimensional (3D) reconstruction and mapping of a scene with overlapping images from different perspectives. Here, we propose a simple method for planning and validating photogrammetric surveys conducted with an ASV. The use of photogrammetry for underwater purposes have been applied by archaeologists since 1968 ([Drap, 2012](#); [Joseph, 1968](#)), and has since been widely adopted in scientific research. Its applications have expanded substantially, particularly in the study of coral reef habitats ([Ferrari et al., 2017](#); [Marre et al., 2019](#); [Million et al., 2021](#)). Most of these studies have focused on small coral colonies with surveys performed by divers, providing accurate estimates of coral surfaces, with errors ranging between 2 to 19% [Lavy et al. \(2015\)](#). Among these, [Marre et al. \(2019\)](#) achieved one of the highest reported resolutions, with an average model resolution of 3.4 mm, demonstrating the potential for fine-scale reef monitoring.

Recently, some studies have explored the use of ASVs for photogrammetry surveys [Johnson-Roberson et al. \(2010\)](#). However, these methods require significant computing resources, which can limit both the accuracy and resolution of the final models. A key challenge is maintaining positional accuracy over a large area, but this can be addressed by coupling images with high-resolution GPS positioning and orientation data. By integrating these additional data sources, photogrammetric models can be run more efficiently and with greater accuracy. Once 3D image reconstruction is complete, orthophotos can then be overlaid onto the bathymetry derived from the echosounder, creating a more detailed and spatially accurate representation of the underwater environment.

Advancements in photogrammetry software have simplified the computing process, reducing the need for extensive preprocessing steps, such as manual camera ordering and calibration. Several software packages are available, but their performance varies depending on survey conditions and image quality, making comparisons difficult [Vlachos et al. \(2019\)](#). For our study, we selected the OpenDroneMap software, which is user-friendly, provides high-quality reconstruction, and also supplies quantitative metrics to evaluate reconstruction quality [OpenDroneMap Development Team \(2025\)](#).

While ASVs provide a promising platform for photogrammetry surveys, they also have limitations. A key drawback using ASVs for photogrammetry of the seafloor is the restricted depth at which the seafloor can be mapped, as visibility is influenced by factors such as ambient light, image quality, turbidity, and surface conditions. These environmental constraints can affect both the accuracy and usability of the collected data.

This paper outlines the tools and methods required to build and operate an ASV equipped with acoustic tracking capabilities as well as integrated bathymetric and photogrammetry data collection.

In the following sections, we describe the ASV's design, covering mechanical, electrical and software components. We then present validation and characterization tests conducted through field surveys, which evaluate each functionality of the ASV and demonstrate the ASV's performance in real-world conditions. Additionally, we provide detailed assembly instructions, hardware specifications, software files, and training datasets in a publicly accessible GitLab repository.⁵

Table 1
ASV requirements for the various operations.

Global	
Handling	2 people recommended
Transport	< 2.5 m (for aircraft regulation)
Deployment	From a small boat or the shore
Environment	Tested in tropical weather: Temp: 10–35 °C
Stance	Stable for wave: 0.5 m / wind: 20 kt
Guidance	Autopilot and manual control
Buoyancy	Can support > 10 kg
Communication	Telemetry range > 1 km
Power limitation	Motor under 2.5 kW
Surveys	
Lifetime per survey	> 2 h
Speed	Between 0.5 and 1.2 m/s
Navigation	Autopilot allow following 1 m transect
Bathymetry sensor	Single beam echo-sounder
Photogrammetry sensor	Camera (e.g. GoPro)
Communication mode	Cellular & telemetry
Tracking	
Lifetime per survey	> 5 h
Speed	about 0.8 m/s
Mechanic	2 m between each hydrophone
Sensor 1	Acoustic geolocation system (SBL)
Sensor 2	Camera for behavior analysis
Communication mode	Cellular & telemetry

2. ASV description

The key requirements for the ASV are summarized in [Table 1](#). The hull is constructed from a paddleboard, selected for the ease of deployment, transportability, and durability in challenging marine conditions. The ASV can be used with or without 3G/4G network, depending on the deployment location, operational needs and available resources. While all functions are operational regardless of internet access, acoustic tracking becomes more challenging without network connection as real-time validation is not possible. The overall network system architecture of the ASV is detailed in [Fig. 4](#).

To ensure affordability and reproducibility, all electronics (except the echosounder) are standard parts commonly used by robotics hobbyists and are readily available from general robotics suppliers.

We divided this section into two subsections: mechanical parts and electronic parts. [Table 2\(a\)](#) summarizes the main components and the total price of each ASV configuration. A complete bill of materials (BOM)⁶ is provided. Additionally, detailed assembly tutorials, wiring diagrams, Computer Aided Design (CAD) files, and installation instructions of the different software components are available in the GitLab repository.⁵

2.1. Mechanical parts

The primary mechanical parts include a paddleboard, a waterproof case for the electronics, and a thruster support positioned underneath the board. Some of the custom parts are 3D printed. For acoustic tracking, additional arms are attached to hold and submerge four hydrophones.

2.1.1. Hull, cases and thruster

The hull is made with a simple paddleboard measuring 87 in length and 80 L in volume. Two thrusters are mounted on a support, which provides stability and protection when the board is on the ground or operating in very shallow waters. This support, made from 5 mm marine-grade aluminum, is designed to be robust and is screwed to the board. To ensure durability and waterproofing, a support base is screwed and bolted on both sides with o-rings. Cables are routed through the board using two custom 3D-printed and coated cable entry points. The echosounder

⁵ GitLab link : <https://gitlab.ifremer.fr/sb07899/Plancha-ASV.git>

⁶ BOM link : https://gitlab.ifremer.fr/sb07899/Plancha-ASV/-/blob/main/Documents/4_BOM.xlsx

Table 2
Description of the main ASV parts for the different configurations and operations.

Global Mode	Component	Name	#	Unit Price in US\$	
(a) Different parts classified by mode and operation					
Electrical	Fligh controller	Pixhawk cube 2.1 black	1	315.00	
	GNSS RTK	Emlid reach M2	1	499.00	
	Telemetry	RFD900	1	277.00	
	Radio command	RadioLink AT9S	1	129.99	
	Thruster	Blue robotic T200	2	179.00	
	ESC	Blue robotic Basic ESC	2	27.00	
	Battery	Tattu 14.8V 25C 4S 10000 mAh	2	149.00	
Remote	GNSS RTK Base	Emlid reach RS2	1	2199.00	
	GNSS radio communication	Reach LoRa radio	1	118.00	
Internet	4G dongle	Huawei E3372	1	50.00	
	Companion board	Raspberry pi 3B +	1	38.00	
Mechanical	Hull	Paddle board 8", 80L	1	250.00	
	Waterproof case	HRDR waterproof case	1	225.20	
	Thruster support	Custom aluminum support	1	150.00	
	Cobalt Series Connector	Blue trail engineering Connector	2	67.00	
Surveys Mode					
Electrical	Echosounder	ETC400	1	3850.00	
	Camera	GoPro Hero 7	1	349.00	
Mechanical	Echosounder holder	Printed custom part	1	20.00	
Tracking Mode					
Electrical	SBL acoustic receiver system	Waterlinked Underwater GPS	1	2200.00	
	Acoustic beacon	Waterlinked locator U1	1	1500.00	
	Additional battery	Tattu 14.8V 25C 4S 10,000 mAh	2	149.00	
Mechanical	Aluminum holding arm	Aluminum tubs	2	200.00	
(b) Price estimation of the ASV for the different modes. Only indicative, it does not include inexpensive components and spare parts					
	Global (G)	G + Surveys	G + Tracking	G + Surveys + Tracking	Remote
Total	~ \$2434	~ \$6634	~ \$6802	~ \$8672	add \$2400

is mounted on a 3D-printed support, which is potted into a pre-drilled hole in the board for secure placement.

All electronic parts and sensors are housed in a waterproof case measuring $54 \times 42 \times 22$ cm. The GPS antenna mast, made of aluminum, functions as a ground plane for the antenna. The echosounder is wired with the Binder 770 Bulkhead Connector and a plug from *Blue Robotics*. For thruster wiring, which requires handling high electrical currents, we chose the Cobalt Series bulkhead connector and plug from *Blue Trail Engineering*.

2.1.2. Integration of acoustic parts

In the acoustic system, we require four hydrophones which are mounted on two aluminum holding arms positioned 2 m apart, following the manufacturer recommendation (see Fig. 2(b)). The first arm, located at the back of the board, consists of five aluminum tubes: two short 10 cm tubes, two 60 cm tubes, and one 2 m tube. The 60 cm and 2 m tubes are connected with a stainless-steel elbow sourced from marine hardware stores. The arm is secured to the board using stainless steel mounting plate, which are screwed onto the surface, and stainless steel T joints to secure the long tube. Bases are screwed onto the board. Since the mounting bases are positioned closer together towards the front of the board, additional reinforcement is necessary. We thus fix the two bases on a 3D-printed support which is then potted on the board. To connect the four acoustic receivers, we used binder 770 bulkhead connectors and plugs from *Blue Robotics*. The connectors are pre-mounted on the acoustic electrical board.

2.2. Electrical parts

For the electrical and software sections, we first described the power part, followed by the main components and sensors. In Fig. 3(b)), elements related to power are represented by a blue background, while the command and sensors are indicated by the green background. The core of this part follows a standard ASV configuration. It includes an autopilot (component 1) for navigation control, a GPS module (component 4) for positioning, and communication systems (component 7) for data transmission and remote operation. All electrical components,

including external sensors (camera, echosounder) and the electronic speed controller (ESC) for the thrusters, are housed in a waterproof case (Fig. 3(c)). Fig. 3(a)) provides an overview of the system, including a high-level electrical schematic and a photograph of the ASV's electrical circuit with annotated labels identifying the corresponding components. Fig. 4 describes the software and how the different components communicate with each other.

2.2.1. Power part

The power part is composed of a minimum of two 4S/10Ah batteries (component 10 - Fig. 3), two electronic speed controllers (ESC) (component 12), two thrusters (component 16), one voltage monitor (component 13), one voltage regulator (component 12) and some fuses. Except for the batteries, all the components are sourced from *Blue Robotics*.

2.2.2. Autopilot

The autopilot or flight controller used in the ASV is the *Pixhawk 2.1* cube black (component 1 - Fig. 3). With the exception of the camera and SBL acoustic system, all ASV components and sensors are connected to the flight controller. The flight controller is powered via the 5 V output of the voltage regulator. A power sense module is integrated into the system to monitor battery voltage and electrical consumption, providing real-time power management. It is also connected to the *Pixhawk*. The flight controller is configured with the open-source autopilot *Ardupilot* rover V3.5 running in "boat" mode. This software manages navigation rules and the configuration of hardware and sensors. The parameters of our configuration are given in the parameter file available in the GitLab repository.⁷

These settings depend on the board selected and the hardware used. Any modifications require recalibration to ensure optimal performance. The autopilot uses the MAVlink protocol, connecting via USB to the companion computer and via radio telemetry to the ground-based computer. A ground control station (GCS) software is required to communicate with and control the autopilot. Different GCSs are available and

⁷ Parameter file path: https://gitlab.ifremer.fr/sb07899/Plancha-ASV/-/blob/main/Software/Parameters/param_110122.param



(a) ASV preparation for a survey operating remotely with the mobile GPS RTK base station (on the yellow tripod)



(b) ASV in acoustic tracking mode

Fig. 2. ASV photos for the different modes: (a) Survey mode for bathymetric and photogrammetric data collection and (b) Acoustic mode for animal tracking with the four arms equipped with hydrophones.

we used *Mission planner* as it displays real-time variables and ASV positions. Mission Planner also allows mission planning and vehicle parameter configuration prior to field deployments (Fig. 5). More information on how to install and use this software is available on the *Ardupilot* website.⁸ A general tutorial about *Ardupilot* rover is available at this link.⁹

2.2.3. Companion computer

The companion computer used in the ASV is a *Raspberry Pi 3B* (component 2 - Fig. 3). It is powered by a 5V voltage regulator. It connects to the flight controller via a USB cable for serial communication. The *Raspberry Pi* has multiple functions, including communicating with the acoustic module and the flight controller, as well as running custom scripts for sensors and ASV components. During tracking mode, the *Raspberry Pi* runs a *Python* acoustic tracking script, which processes data from the flight controller and the acoustic modem. In internet mode, the *Raspberry Pi* connects to the network using a USB 4G dongle, allowing

it to act as a WiFi access point to share its connection. To enable remote access, we use OpenVPN, which allows secure SSH connections to the *Raspberry Pi* via the internet. More information on how to use *Raspberry Pi* as companion computer is available.¹⁰ Detailed information and the procedure to install the *Raspberry Pi* image are available on the GitHub repository.¹¹

2.2.4. RTK GNSS

We use an *Emlid Reach M2*¹² as a differential GNSS receiver (component 4) with the possibility of Real Time Kinematics (RTK) (Fig. 3). It connects to the flight controller via serial communication through a telemetry port. The *ReachM2* is powered with a micro USB connector connected to a 5V voltage regulator. The *ReachM2* can be configure via WebGui or a smartphone app. In internet mode, the GNSS connects to the WiFi access point of the companion computer, allowing it

⁸ <https://ardupilot.org/copter/docs/common-choosing-a-ground-station.html>

⁹ <https://ardupilot.org/rover/docs/rover-first-drive.html>

¹⁰ <https://ardupilot.org/dev/docs/raspberry-pi-via-mavlink.html>

¹¹ Software instructions link : https://gitlab.ifremer.fr/sb07899/Plancha-ASV/-/blob/main/Documents/2_software_instructions.docx

¹² <https://store.emlid.com/product/reachm2/>

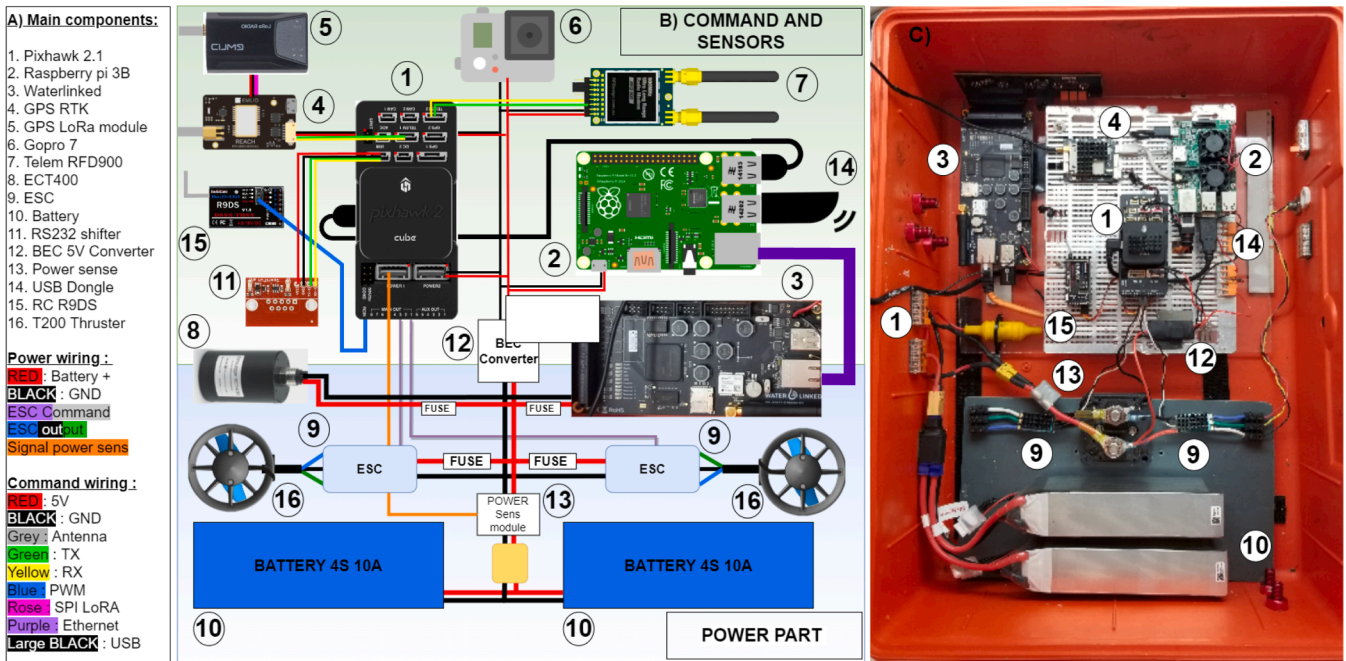


Fig. 3. ASV high level electrical schematic and electrical circuit. On the left (A), the corresponding numbers and names of the main parts. The colored names correspond to different wires on the electrical diagram. In the middle panel (B), the high level electrical schematic displays the main components and wiring. On the right (C), the electrical circuit with the corresponding numbers. Some components are fixed on the top of the case or outside and thus are not visible in this photo.

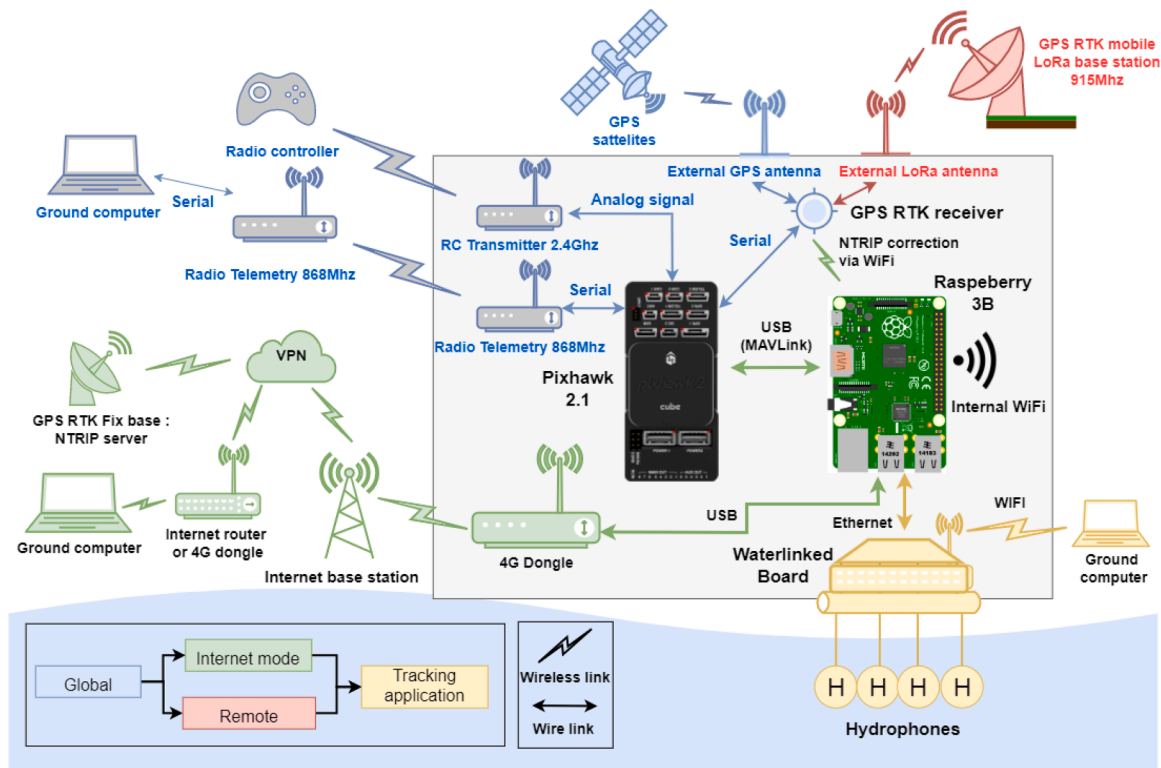


Fig. 4. Network diagram of the ASV showing how the autopilot receives and interacts with the difference sources of information to perform the navigation of the ASV.

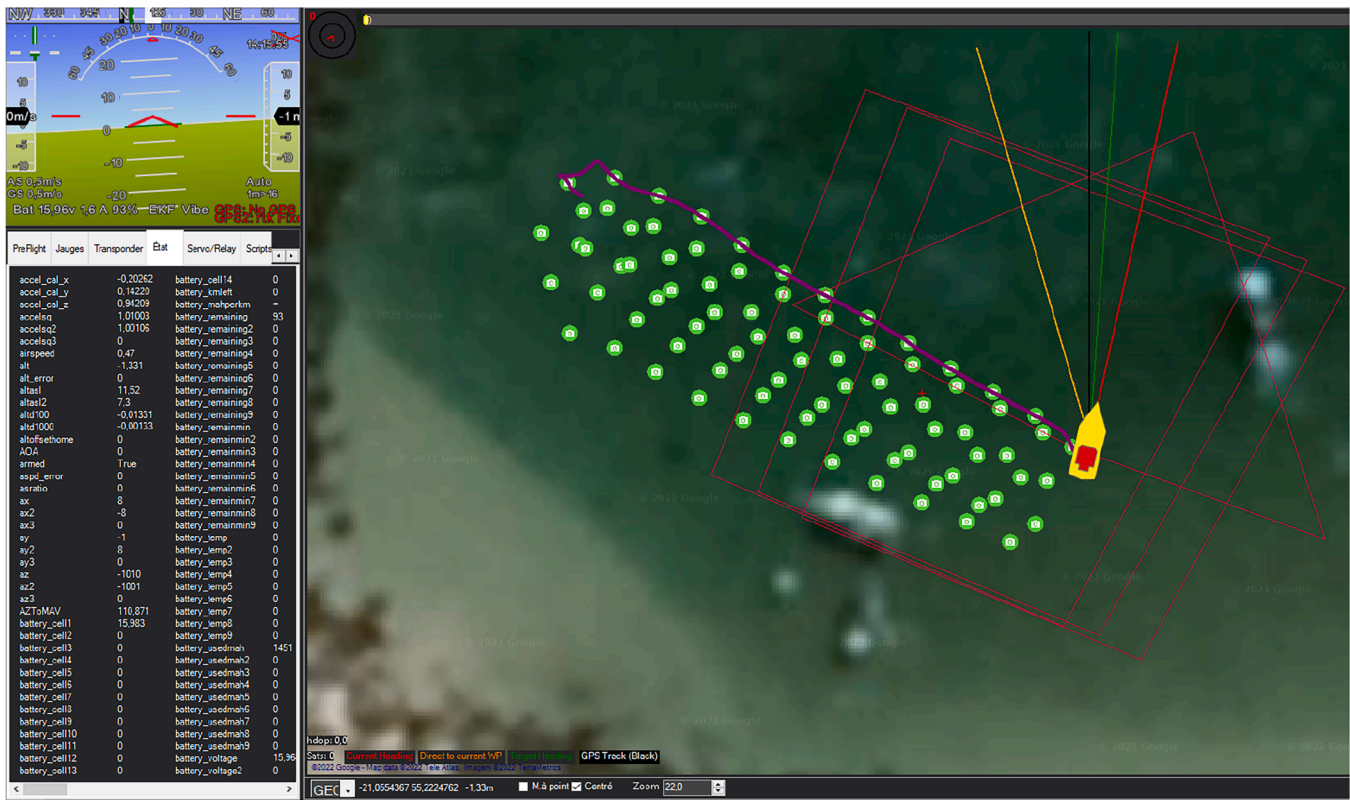


Fig. 5. Screenshot of Mission Planner during a navigation test in Saint-Gilles les Bains (Reunion Island). The yellow boat shape corresponds to the ASV position. The purple line is its actual track and the green dots are positions where an external signal is sent to control a camera. (For interpretation of the references to color in this figure legend, the reader is referred to the web version of this article.)

to fetch corrections through an online NTRIP server (for example, using the docker available here¹³). For remote mode, RTK corrections are transmitted using a LoRa link. In this case, a second GNSS receiver is deployed as a reference base and sends RTK corrections to the embedded GNSS. For this purpose, we use an *Emlid* RS2 located at a known reference position. The complete setup of the GNSS module is available in the *Emlid* documentation.¹⁴

2.2.5. Communication

Several methods of communication are available for telemetry. Here, we primarily use radio telemetry or an internet connection, with radio telemetry serving as a reliable backup even in internet mode. The radio telemetry system (component 7 - Fig. 3) facilitates communication between the autopilot and the GCS software via the mavlink protocol. For this, we chose the RFD900x module operating at 868 MHz, which provides a communication range of 20 km. It ensures a reliable link with the ASV and it is used in both modes.

In manual mode, the ASV can be controlled using a radio control (RC) transmitter to perform some simple tasks such as arming and disarming the thrusters. We use the R9DS RC model operating at a radiofrequency of 2.4 GHz, with the RC receiver (component 15 - Fig. 3) connected to the RCIN port of the flight controller. The RC radio transmitter is used as a fail-safe backup in case of telemetry or internet connection failures.

2.3. Additional sensors

2.3.1. Echosounder

The echosounder used for the ASV is the ECT400 by *Echollogger* (component (8)). It is an echosounder with a single-beam frequency capable

of conducting bathymetric surveys at depths of up to 100 m with a 5° beam angle. The ground and power wires of the echosounder are connected to the battery output as it supports a wide power voltage range (8 to 75 VDC) and thus does not require any voltage regulation.¹⁵ For data transmission, the echosounder communicates with the flight controller via a serial link and an RS232 level shifter is used to convert the output of the echosounder to a 5 V serial signal. The recorded depth data are stored in the ardupilot log as the “DPTH” variable. The echosounder must be configured as described in the *Ardupilot* tutorial.¹⁶

2.3.2. SBL acoustic positioning

The SBL system used in our setup is the underwater GPS G2 from *Waterlinked* R100 (component (3)). It consists of four acoustic receivers, a master board, and an acoustic beacon. The electrical board is connected to the *Raspberry Pi* using an Ethernet cable. The input voltage range is between 10 and 30 V. We connected the board directly to the battery voltage by adding a 3 A fuse. The acoustic transmitter used in the system is the locator U1, which must be manually activated and has battery life of 10 h. The standard version of the SBL system has a range of 100 m, with positioning accuracy 1 % of the range, i.e., 1 m for this application. A WebGui is available to configure the underwater GPS. The acoustic receiver array needs a specific baseline configuration.¹⁷

Waterlinked recommends maintaining a distance of 2 m between each acoustic receiver. Distances between the acoustic receivers are measured directly on the paddleboard and entered into the baseline configuration tab using the WebGUI. For our application, orientation and position data

¹³ <https://github.com/goblimey/ntripcaster>

¹⁴ <https://docs.emlid.com/reach/reachview-3/connecting-to-reach>

¹⁵ <https://www.echollogger.com/products/single-frequency-echosounder-deep>

¹⁶ <https://ardupilot.org/copter/docs/common-echollogger-ect400.html>: Configuring the sensor

¹⁷ <https://store.waterlinked.com/product/locator-u1/>

are retrieved from the flight controller and transmitted by the companion computer. The settings “tab/top-side”, GPS and compass must be switched to *External*. To record the tracking data, we use a custom *Python* script, which runs on the companion computer and logs tracking information. The software and system integration information are explained in the documentation.¹⁸ For our specific application, the procedure details are available in documentation folder.¹⁹

The position of the acoustic transmitter to the ASV is calculated using a time of arrival algorithm to calculate the signal arrival times between each different receiver to determine the relative position. The system then integrates the GPS position and heading of the ASV to calculate the geolocated position of the transmitter. To keep the acoustic receiver within the 100 m operational range, its position is continuously defined as a new waypoint, guiding the ASV.

2.3.3. Camera

We used the *GoPro 7* black edition (component (6)) as the onboard camera powered by a 5V voltage regulator. The camera’s images play a crucial role in both photogrammetry and tracking modes. For photogrammetry, the *GoPro 7* is mounted to face downward, whereas in tracking mode, it is mounted at a 30° angle from the vertical position. During the photogrammetric survey, the field of view of the *GoPro 7* should be as linear as possible to ensure accurate reconstruction of 3D images. To optimize image quality, we set the ISO parameter at the lowest value (ISO 100) and the shutter speed at a high value. The *GoPro 7* is set in video mode to ensure continuous image capture. A minimum of at least 70 % overlap is required between two pictures for reliable photogrammetry results. We used an excel file²⁰ to calculate the space between transects as a function of the depth of the survey area and the coverage needed. The distance between transects also highly depends on the navigation accuracy capabilities of the ASV.

3. Prototype validation and survey results

To illustrate the potential applications of the ASV, we present some survey results. The validation of the ASV (e.g. accuracy of the trajectory) and the power consumption estimates are provided in the Git repository.²¹ All data and software presented in the section are available here.²²

3.1. Autonomous acoustic tracking

The acoustic tracking feature allows for fine-scale trajectory estimation and active tracking of the underwater acoustic beacon (U1 Locator). The beacon measures 3.2 cm × 12.1 cm, and weighs 75 g in water. This tracking feature can be applied to various use cases such as tracking AUVs or monitoring animals/humans with limited swimming speeds. For ethical reasons, preliminary prototype tests were conducted on divers and were later conducted with wild animals. For the first case study, the beacon was deployed on a freediver instructed to mimic the surfacing behavior of a turtle. The survey was conducted at Cap Lahoussaye (21.0173°S, 55.2382°E). Once the prototype was validated, we deployed the system on a wild juvenile green turtle in a second experiment off Saint-Gilles-les-Bains (21.0571°S, 55.2194°E). The tagging process followed a standardised protocol reviewed by an ethical committee and local regulations, with all personnel involved receiving comprehensive training (see Section 4). The following subsections detail the

tracking procedure, data processing, and the results obtained from these two case studies.

3.1.1. Protocol

Tracking. The *WaterLinked* system does not store the trajectory but only displays it on their WebGui. In their GitHub repository,²³ *WaterLinked* provides example scripts in *Python* for data retrieval and logging, executable directly from a laptop. To enable tracking and data logging for our purposes, we developed our own logging scripts tailored to the needs of this study,²⁴ *WaterLinked*. Furthermore, we developed a tracking algorithm to calculate waypoints and transfer them to the autopilot. To initiate the tracking mode, the user must run a command. The algorithm operates as follows: the ASV’s position and heading are retrieved from the flight controller; these data are then sent to the SBL module to estimate the position of the acoustic beacon. The *Raspberry Pi* queries the beacon’s position and compares it to the ASV’s location. If the ASV and beacon are too close (5 m), the autopilot switches to hold mode. If the beacon moves beyond a threshold distance (set to 15 m), a new waypoint is sent to the autopilot to pursue the target. Navigation rules update the distance between the ASV and the beacon every second. Tracking parameters are logged on the *Raspberry Pi*.

Tagging. The U1 Locator was attached on the diver’s chest with a 50 cm offset towards the seabed to ensure it remained submerged when the diver surfaced, minimizing acoustic signal loss. Despite this adjustment, occasional signal spikes and losses were observed when the diver surfaced. For the turtle experiment, the acoustic beacon was attached to the shell of the turtle’s back. During surfacing events, the beacon was temporarily exposed above the water, causing loss of signal.

3.1.2. Data processing

Tracking data, including the 3D positions of the ASV and acoustic beacon, were logged on the *Raspberry Pi*. Custom *MATLAB*©scripts were developed for data analysis, filtering, and visualization. The acoustic sampling frequency was set to 1 Hz. To estimate tracking accuracy, we used the standard deviation (STD) of position estimates provided by the system. To obtain an accurate trajectory, positions with a standard deviation exceeding 3 m were removed. A linear interpolation was applied to refine the acoustic track. The complete filtering procedure is documented in our Git repository.²⁵

3.1.3. Results

Freediver tracking. Fig. 6 presents a 25-min tracking sequence of a freediver. The system successfully tracked and calculated the diver’s 3D position. These results validate the method and demonstrate the potential of our ASV to calculate and record precise underwater positioning of a moving target, which can serve as reference data for diverse marine tracking applications, including the study of animal movements, diver safety monitoring, and AUV navigation.

Wild turtle tracking. During the second experiment with a wild turtle, tracking was maintained for 228 min. The average power consumption was 7.05 A, suggesting that with the 40 Ah battery, tracking could have continued for an additional 30 min. After filtering, a valid fine-scale trajectory of 138 min was calculated from the tracking data (60 % of the total recording time). Fig. 7(a) illustrates the tracking results and Fig. 7(b) plots the ASV-turtle distance alongside the STD of the signal, with annotated phases for analysis (see text for the description of the different phases).

¹⁸ <https://waterlinked.github.io/underwater-gps/quickstart/>

¹⁹ Documentation folder : https://gitlab.ifremer.fr/sb07899/Plancha-ASV/-/blob/main/Documents/2_software_instructions.docx

²⁰ https://gitlab.ifremer.fr/sb07899/Plancha-ASV/-/blob/main/Software/Photogrammetry/Spacing_between_transect_calculator.xlsx

²¹ Illustration examples link: https://gitlab.ifremer.fr/sb07899/Plancha-ASV/-/tree/main/Features_example/test_conso_18_02_22

²² Illustration examples link: https://gitlab.ifremer.fr/sb07899/Plancha-ASV/-/tree/main/Features_example

²³ <https://github.com/waterlinked/examples>

²⁴ Tracking and communication scripts: https://gitlab.ifremer.fr/sb07899/Plancha-ASV/-/tree/main/Software/Tracking?ref_type=heads

²⁵ Filtering procedure: <https://gitlab.ifremer.fr/sb07899/Plancha-ASV/-/tree/main/Documents>

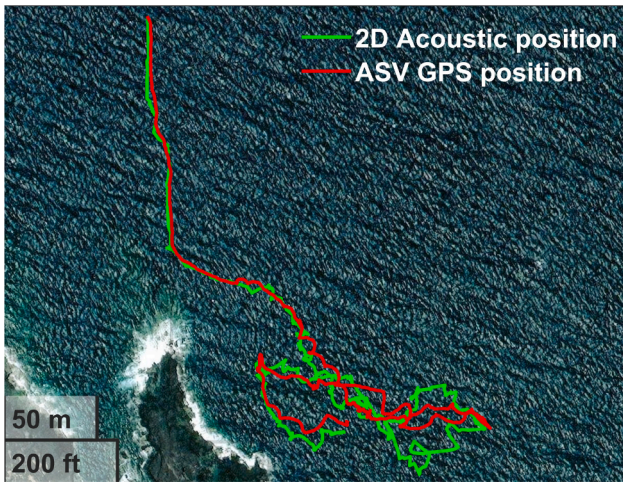


Fig. 6. ASV tracking of a freediver. Green track is the underwater acoustic position. Red is the ASV position.

Phase 1. Turtle release. Initially, the turtle exhibited fast swim escape, staying near the surface. The ASV struggled to maintain tracking and lost the acoustic signal. At around 211 s, the ASV reacquired the signal approximately 80 m from the target when the turtle performed a deeper dive, thus allowing the tracking to restart.

Phases 2, 4, 6 and 8. Normal tracking phases. During these phases, tracking proceeded as expected. Shaded areas correspond to resting phases on the seafloor. During these phases, the ASV maneuvered to the turtle's position, entered hold mode, and drifted with the current (regular hatched pattern, Fig. 7(b)).

Phases 3 and 7. Tracking was interrupted twice due to signal loss between the ASV and the acoustic modem (for 871 s and 726 s). In phase 7, the turtle was resting on the seabed, allowing easy reacquisition of the signal. During phase 3, the turtle was in motion, and the ASV was approximately 40 m away when the acoustic module restarted. It took 308 s for the ASV to catch up with the turtle and return to the predefined tracking distance. Excluding technical failures timing, 72% of tracking was valid. An improvement to the tracking algorithm could involve implementing a search pattern upon signal loss.

The overall mean STD on turtle position was 6.93 m. During normal tracking (excluding technical issues and signal loss), the mean STD was 1.80 m. Every surfacing event resulted in STD spikes due to a loss of precision as the beacon emerged from the water. However, since the turtle remained stationary during surfacing, tracking was not significantly affected. Fig. 7(c) plots the ASV-turtle distance against the mean STD. We use a moving median filter to smooth the noise of the STD data, removing outliers caused by spikes from poor acoustic reception. To maintain an average STD of 3 m or less, the ASV should be positioned between 4.7 m and 14 m horizontal distance from the animal. Higher STD values at close distances likely come from issues with the acoustic signal triangulation when the ASV's receivers are directly above the beacon. For horizontal distances beyond 40 m, data were insufficient to draw conclusions, though the STD remained below 10 m.

These results provide a precise fine-scale trajectory of a wild marine turtle's movements, which can be used to address ecological questions including behavioral mapping of the animal's movement within its environment (Fig. 8).

Video analysis. The quality of video data depends on underwater visibility and the proximity of the camera to the target. Unfortunately, during the second experiment, visibility was low and we were not able to collect enough footage of the turtle within the camera's field of view. Fig. 9

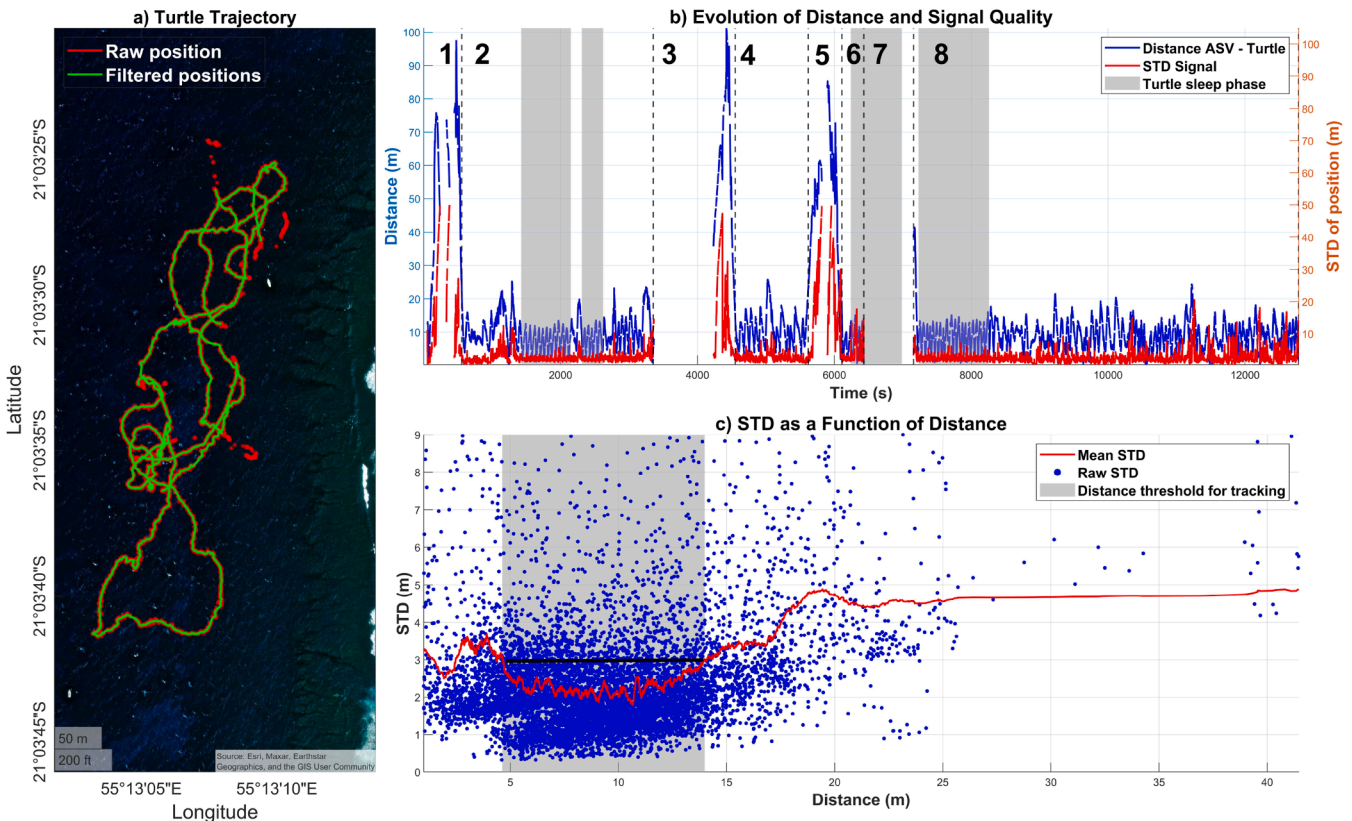


Fig. 7. (a) Underwater trajectory of the tagged sea turtle on satellite map. (b) Plots the ASV-turtle distance alongside the standard deviation of the distance (STD) with the different phases annotated by a number for subsequent analysis. (c) STD in function of distance between the ASV and the turtle.

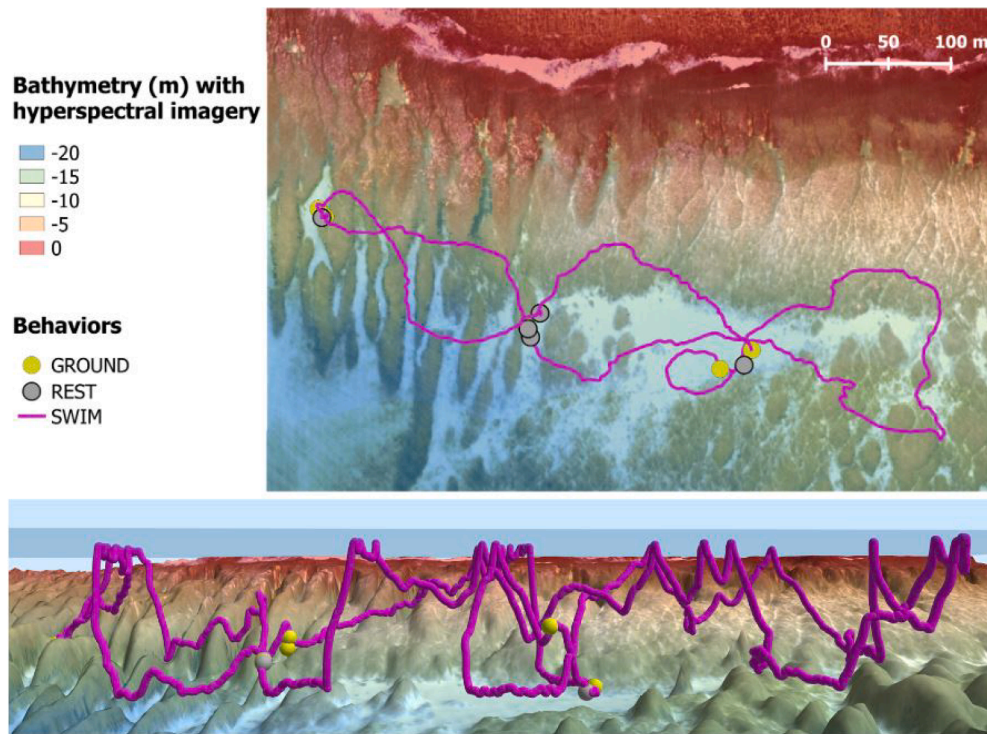


Fig. 8. Example of a map with a turtle's trajectory and behavior sampled with the ASV (top). The same data are shown in 3D (Bottom). The layers displayed are single beam bathymetry associated with hyper-spectral imagery of the area.



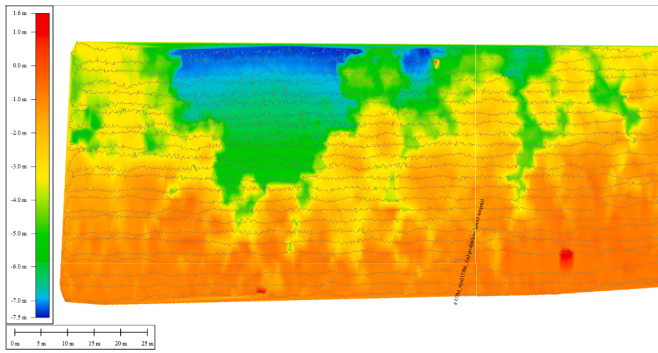
Fig. 9. Screenshot of the GoPro 7 footage during the second tracking experiment when the turtle is diving. Behavioral analyses based on video images are limited in our experiment due to low visibility.

shows a snapshot of the turtle when it was close to the ASV (5 m), where it is barely visible.²⁶

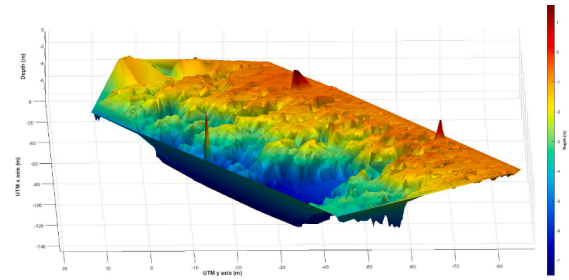
²⁶ Processing script in git: https://gitlab.ifremer.fr/sb07899/Plancha-ASV/-/blob/main/Features_example/test_tracking_26_10_21/code/main_acoustic_tracking_20_10_21.m

3.2. Bathymetry survey

Information extracted from bathymetric data depends not only on sensor specifications, but is also on the seafloor topology and spacing between collected points. Key parameters such as the maximum measurement range, sampling frequency, and sensor errors were fixed



(a) Computed sea depth map with overlaid ASV paths (grey lines). Map generated with Global Mapper®



(b) The same bathymetric data are used to generate a 3D-projection using Delaunay triangulation. Plot generated with MATLAB

Fig. 10. Bathymetry results of a survey done in 2020 in Europa Island (22.3406°S, 40.3381°E) with the ASV.

during the design phase. However, for each survey, prior knowledge of the seafloor topology is essential to optimise the spatial distribution of the data collection over the survey area. Information such as average depth and type of substrate (e.g. large rocks, sand rift, corals, ...) will help when planning the spacing between points. The spacing between transects must also be adapted to the desired resolution of the map.

Several standards are available that assist in defining the objectives of bathymetric surveys and classifying the quality of their results. To define the specifications of our bathymetric surveys, we use the standards proposed by the International Hydrographic Organization Organization (2020) (section 7.3, Table I) that are based on the overall accuracy, the area coverage, and the types of features that can be detected.

The next sections present the protocol, the processing stages, and the final results for a bathymetric survey with an illustration from a survey carried in 2020 on the north shore lagoon of Europa island in the Mozambique Channel.

3.2.1. Protocol

Based on the requirements outlined in Standards for Hydrographic Surveys Organization (2020) and detailed in the Supplementary Materials, our surveys fall under *order 1a* category. This classification applies to data collected in harbors, harbor approach channels, coastal areas or inland navigation channels, with the limitation that is restricted to areas with depths less than 100 m.

The survey site was a lagoon in Europa Island (22.3406°S, 40.3381°E). Bathymetry in this area has been previously estimated using hyperspectral and LiDAR data collected by the Litto3D Océan Indien project in 2019²⁷ (see Section 3.2.3) and shows depths ranging from 1 m to 10 m.

To meet the *order 1a* bathymetry standard, we defined the survey area as a rectangle of 49 m × 115 m, centered at 22.340984°S, 40.337634°E. The ASV autopilot parameters were configured as follow:

- 24 transects aligned along the widest dimension, with 2-m spacing between transects;
- a target cruise speed of 1 m/s;
- a depth sampling rate of 2 Hz.

These settings result in a grid of 24 × 228 points across the survey zone. The resulting *bathymetric pixels* have diameters ranging from 9 cm to 90 cm, depending on depth (1–10 m). The pixels spacing is 0.5 m width-wise and 2 m lengthwise.

²⁷ Data accessible here: <https://oceans-indien-austral.milieuamrinfra.fr/Access-aux-Donnees/Catalogue#/metadata/6b796349-d56e-44c3-b572-d5488250637e>

3.2.2. Data processing

The survey data are retrieved from the autopilot log file, which contains all recorded system information, statuses and measurements collected by the ASV during the survey. The first step in data processing is to discard any unnecessary data and keep only the echo-sounder, GPS, and inertial measurement unit data over the survey area. For an accurate depiction of the seabed, pre-processing is required to correct and filter the measured depth values. The raw data processing workflow includes the following steps:

- Attitude filtering: using the ASV's attitude data (roll, pitch, yaw) given by the IMU sensor, any points where the pitch and roll angles exceed 10° are removed.
- Outlier removal: A sliding median filter is applied to eliminate outlier depth values based on the median depth computed within a sliding window.
- GPS position correction: the position offsets between the GPS antenna and the location of the ASV's echosounder are corrected along the three axes.
- Depth location adjustment: the true seabed location of the measured depth is determined by correcting the surface GPS positions with the ASV attitude.
- Final depth correction: the recorded depth values are corrected with the ASV attitude, the local datum, and the geoid model of the survey zone, to obtain a compensated and georeferenced depth map.

A minimal working example in *Python* is available on the Git repository associated with this article.²⁸

3.2.3. Results and comparison with prior data

For the survey mentioned above, Fig. 10 shows different depth estimates of the same pre-processed data set. In Fig. 10(a), the depth map has been automatically computed using the *Global Mapper*® software. Overlaid gray lines represent the ASV path extracted from raw GPS data collected during the survey. These data are visualised in a 3D projection (Fig. 10(b)) constructed using *MATLAB*.²⁹

We compare three different techniques that have been used to analyze the sea floor of the Europa lagoon (Fig. 11) to illustrate the benefits of using a single-beam echosounder on an ASV. The maps presented correspond to a subset of the survey area discussed above. Fig. 11(a) shows the satellite imagery of the surveyed area. Fig. 11(b) presents the ASV

²⁸ Example bathymetric data processing script in git : https://gitlab.ifremer.fr/sb07899/Plancha-ASV/-/blob/main/Software/Bathymetry/Compute_depth.py

²⁹ Example script in git : https://gitlab.ifremer.fr/sb07899/Plancha-ASV/-/blob/main/Features_example/test_bathy_europa_09_10_20/code/main_plot_bathy_09_10_20.m

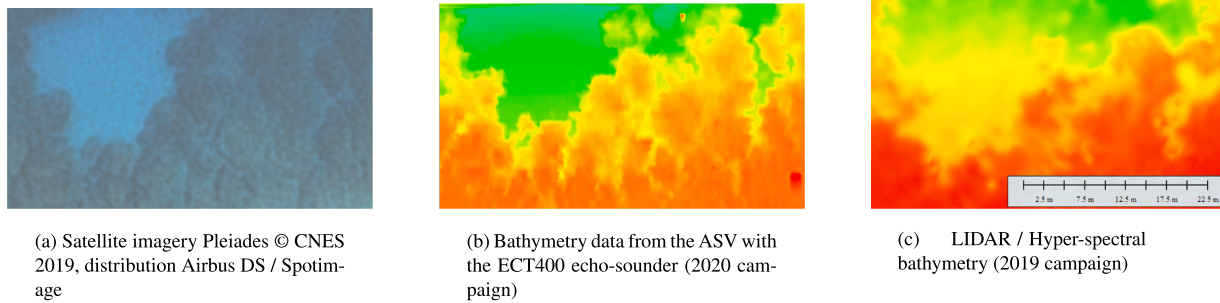


Fig. 11. Three different methods to represent the sea floor in the survey area located inside the Europa's lagoon.

bathymetry data of a zoomed-in view of the previous map shown in Fig. 10(a). Fig. 11(c) shows the bathymetric data estimated from hyper-spectral and LiDAR data collected from the same area in 2019 (Litto3D Océan Indien project).

A strict quantitative comparison of feature resolution and depth accuracy among the three methods discussed is outside the scope of this paper. Such analysis would require careful consideration of factors including the different geodesic reference frames used, the level of depth correction applied, the inclusion of environmental/experimental parameters (i.e. temperature, salinity, the effect of tides, ...), and interpolations errors introduced by the varying spatial distribution of each dataset.

However, we find that a qualitative analysis is sufficient to confirm that the ASV bathymetry provides an accurate representation of the seabed topology in this area when compared to the satellite imagery. The ASV bathymetry aligns well with the hyperspectral/LiDAR data, but offers greater detail due to higher resolution. While aerial hyper-spectral techniques have the advantage of covering large areas quickly, ASVs equipped with single-beam echosounders provide a more cost-effective and practical solution for high-resolution mapping of smaller areas. Additionally, using an ASV instead of a boat has several advantages, including more regular and dense sampling patterns, improved maneuverability of shallow or otherwise inaccessible zones, and lower operation costs for small areas.

3.3. Photogrammetry survey

Images collected over the survey area can be used to generate photogrammetric models. As the ASV is equipped with a differential GPS and an autopilot system that records positioning and attitude information, each image contains metadata that significantly improve the reconstruction accuracy of the photogrammetric model Contini et al. (2025a). Here, we describe the protocol, data processing methods, and results of these surveys.

3.3.1. Protocol

Camera calibration is essential to optimize photogrammetric reconstruction results. To mitigate lens distortion, the lens and sensor parameters of the GoPro camera must be accurately estimated. Calibration can either be computed automatically by photogrammetry software or manually estimated by capturing multiple images of a 9×7 square chessboard pattern from varying positions and angles. OpenDroneMap includes a built-in calibration procedure to calculate and store the camera model. To achieve a three-dimensional reconstruction of the survey area, each image must overlap adjacent images by at least 70%, photos must be clear, free of surface reflections on the seabed, and without shadows from the ASV. Using survey-specific data and camera characteristics (e.g., camera field of view, water depth), it is possible to calculate the optimal distance between transects to satisfy the required overlap. We developed a tool to estimate this distance.³⁰ Note that this calculation

does not include camera sampling frequency or ASV speed. For the examples provided in this paper, the ASV speed was set at 1 m/s, with a transect spacing of 1 m, in survey areas ranging from 0.6 m to 7 m depth.

3.3.2. Data processing

Underwater images used for photogrammetric reconstructions were extracted from videos captured with GoPro cameras. Videos were split into frames at regular time intervals, and timestamps were used to synchronize GPS positions and images. Further details on image processing are described in Contini et al. (2025b). As OpenDroneMap leverages GPS positioning and attitude metadata (roll, pitch, and yaw) to enhance reconstruction results, these metadata were provided for each image. Further information on image footprint calculations on the seabed is provided by Contini et al. (2025a).

3.3.3. Results

Fig. 12 illustrates photogrammetric reconstruction results derived from 9143 images captured in Reunion Island. Despite all images being captured from the sea surface with minimal angular variation relative to the seabed (mainly due to wave-induced motion), effective three-dimensional reconstructions were achieved, clearly revealing geological faults, coral communities, and features such as wrecks colonized by coral. We evaluated four photogrammetry datasets collected in St. Leu, Reunion Island (21.1638°S, 55.2863°E), to assess reconstruction accuracy and processing quality. Each dataset covered an average area of 6,182 m² using approximately 9231 images. Positioning accuracy of the reconstructed models was evaluated using two metrics: horizontal accuracy CE90 (radius containing 90% of points horizontally) and vertical accuracy LE90 (vertical difference encompassing 90% of points). These metrics were calculated using two approaches:

- **Absolute accuracy**, including intrinsic GPS error;
- **Relative accuracy**, comparing GPS data and reconstructed values without considering GPS systematic errors.

Table 3 summarizes the accuracy results. Although absolute accuracy shows huge deviations, the relative accuracy values are within centimeters, indicating high internal consistency in reconstructed models. Improvements on the absolute accuracy can be obtained by means of Ground Control Points (GCPs) Contini et al. (2025a).

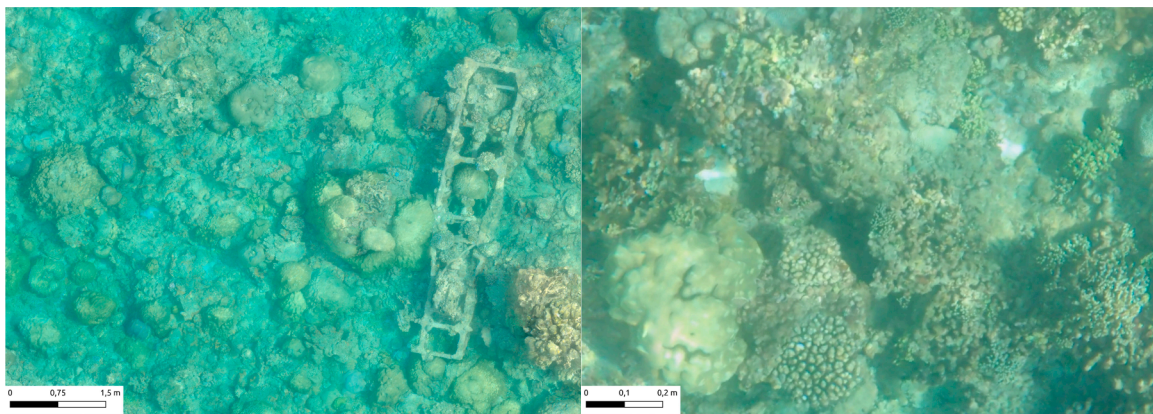
Detailed GPS and 3D reconstruction errors (mean, standard deviation, RMS) for each session are provided in session-specific photogrammetry reports, available with open-access via Zenodo Bonhommeau et al. (2024a,b,c,d).

Table 3

Average absolute and relative accuracy metrics.

Accuracy type	Absolute mean (m)	Relative mean (m)
Horizontal accuracy CE90	0.513	0.006
Vertical accuracy LE90	0.663	0.013

³⁰ https://gitlab.ifremer.fr/sb07899/Plancha-ASV/-/blob/main/Sotfware/Photogrammetry/Spacing_between_transect_calculator.xlsx

(a) Top-view orthophoto reconstruction covering 5,733 m².

(b) Zoomed view of a wreck colonized by coral.

(c) Zoomed view of diverse coral assemblages.

Fig. 12. Photogrammetric reconstructions from 9143 images captured by the ASV during a 2024 survey in Reunion Island (21.1638°S, 55.2863°E).

4. Conclusion

This paper fully describes the hardware, software, and data processing tools for an ASV. The ASV is able to perform:

- autonomous navigation with an autopilot;
- autonomous acoustic tracking with an acoustic SBL system;
- bathymetric surveys with a single beam echosounder for depth < 50 m; and
- photogrammetric surveys with a low-cost camera.

All components and mechanical parts were selected to be low-cost, readily available, and easy to assemble. The software, firmware, flight controller, and in-house development are open-source, ensuring accessibility and adaptability.

The ASV is not designed for use in rough seas or weather conditions. Field tests have shown that the ASV can flip in windy conditions (> 20 kt) and choppy waves (≈ 0.3 m). It is advised to be operated by two operators in case of an issue where the board needs to be recovered.

In addition to the system description and validation, we provide a Git repository containing all necessary documents, assembly instructions, and software files to replicate this ASV. The ASV is adaptable to different environmental conditions and can operate with or without internet. The radio telemetry system enables control of the ASV within a range of a few kilometers. For inhabited coastal regions with stable internet coverage, such as Reunion Island, the ASV remains connected throughout the survey (< 1 km from the coastline). The ASV is powered by two 2S batteries (10 Ah each), providing over 4 h of survey time. These batteries comply with air transportation regulations, making it possible to transport the ASV in a surf bag for ease of travel.

To summarize, the ASV is reliable, easy to use, reproducible, and customizable. Its compact and lightweight design makes it easy to transport and practical for field deployments. With telemetry and ground control software, the ASV can be monitored with a laptop in real-time during surveys. The software enables users to create survey missions, adjust parameters, and calibrate the ASV as needed. Additionally, the *ArduPilot* flight controller logs mission data and facilitates post-survey analyses with the dedicated tools.

The ASV's high buoyancy and available deck space allow for the integration of other sensors, batteries, or new functionalities. Thanks to the *Raspberry Pi* companion computer and the *Pixhawk 2.1* flight controller running *ArduPilot*, integrating new software components is straightforward and adaptable to different applications.

These features demonstrate that low-cost ASVs can effectively support environmental and ecological monitoring, providing high resolution data at an accessible cost. To our knowledge, this is the first ASV to track an acoustic beacon using a low-cost SBL system. This ASV is capable of recording accurate, fine-scale underwater animal trajectories, even at shallow depths, while simultaneously collecting bathymetric and photogrammetric data.

Ethical statements

Tagging has been approved by an ethical committee for animal experiment (APAFIS#26501-2019111414383771 v2) and by the National Council for Nature Protection (2020-00664-031-001). The authorization to tag sea turtles in the Marine Reserve of Reunion Island has been approved by the Prefet de la Réunion (DECISION N°2020-45 and DECISION DEAL/SEB/UBIO/2022-08).

Declaration of competing interest

The authors declare that they have no known competing financial interests or personal relationships that could have appeared to influence the work reported in this paper.

CRedit authorship contribution statement

Pierre Gogendeau: Writing – original draft, Visualization, Validation, Software, Methodology, Investigation, Formal analysis; **Sylvain Bonhommeau:** Writing – review & editing, Supervision, Project administration, Investigation, Funding acquisition; **Hassen Fourati:** Writing – review & editing, Supervision; **Mohan Julien:** Visualization, Investigation; **Matteo Contini:** Investigation; **Thomas Chevrier:** Investigation; **Anne Elise Nieblas:** Resources; **Serge Bernard:** Writing – review & editing, Supervision, Methodology, Funding acquisition.

Acknowledgment

We are grateful to Steven Le Bars and Vincent Macaigne from ID OCEAN for their support and loan of material. Thanks to Andrea Goharzadeh, Denis De Oliveira, Geoffrey Fournier, Pauline Salvatico and Julien Fezandelle for their help in the project. Thanks to Pascal Mouquet for the satellite images. Finally, we thank *Emlid* and *Blue Robotics* for the use of some of their images. This work is supported by the “IOT” project funded by FEDER INTERREG V and Prefet de La Réunion: under Grant 20181306-0018039 and the Contrat de Convergence et de Transformation de la Préfecture de La Réunion.

References

Baldi, S., Sun, D., Xia, X., Zhou, G., Liu, D., 2022. ArduPilot-based adaptive autopilot architecture and software-in-the-loop experiments. *IEEE Trans. Aerosp. Electron. Syst.* 58 (5), 4473–4485. Conference Name: IEEE Transactions on Aerospace and Electronic Systems. <https://doi.org/10.1109/TAES.2022.3162179>

Bonhommeau, S., Barde, J., Contini, M., 2024a. Underwater images collected by an Autonomous Surface Vehicle in St-Leu, Réunion - 2023-11-10. <https://doi.org/10.5281/zenodo.12760540>

Bonhommeau, S., Barde, J., Contini, M., 2024b. Underwater images collected by an Autonomous Surface Vehicle in St-Leu, Réunion - 2023-11-10. <https://doi.org/10.5281/zenodo.12760678>

Bonhommeau, S., Barde, J., Contini, M., 2024c. Underwater images collected by an Autonomous Surface Vehicle in St-Leu, Réunion - 2023-11-10. <https://doi.org/10.5281/zenodo.12760930>

Bonhommeau, S., Barde, J., Contini, M., 2024d. Underwater images collected by an Autonomous Surface Vehicle in St-Leu, Réunion - 2023-11-10. <https://doi.org/10.5281/zenodo.12760125>

Boogie Board Boat, 2022. Boogie board boat — rover documentation. <https://ardupilot.org/rover/docs/reference-frames-boogieboard-boat.HTML>

Carlson, D.F., et al., 2019. An affordable and portable autonomous surface vehicle with obstacle avoidance for coastal ocean monitoring. *HardwareX* 5. Publisher: Elsevier. <https://doi.org/10.1016/j.ohx.2019.e00059>

Campos, D.F., Gonçalves, E.P., Campos, H.J., Pereira, M.I., Pinto, A.M., 2024. Nautilus: an autonomous surface vehicle with a multilayer software architecture for offshore inspection. *J. Field Robot.* 41 (4), 966–990. [_eprint: https://doi.org/10.1002/rob.22304](https://doi.org/10.1002/rob.22304)

Chambault, P., Dalleau, M., Nicet, J.-B., Mouquet, P., Ballorain, K., Jean, C., Ciccione, S., Bourjea, J., 2020. Contrasted habitats and individual plasticity drive the fine scale movements of juvenile green turtles in coastal ecosystems. *Mov. Ecol.* 8 (1), 1. <https://doi.org/10.1186/s40462-019-0184-2>

Chaysri, P., Spatharis, C., Vlachos, K., Blekas, K., 2024. Design and implementation of a low-cost intelligent unmanned surface vehicle. *Sensors* 24 (10), 3254. Number: 10 Publisher: Multidisciplinary Digital Publishing Institute. <https://doi.org/10.3390/s24103254>

Contini, M., Illien, V., Barde, J., Poulain, S., Bernard, S., Joly, A., Bonhommeau, S., 2025a. From underwater to aerial: a novel multi-scale knowledge distillation approach for coral reef monitoring. *arXiv preprint Preprint, not peer-reviewed.* 2502.17883. <https://arxiv.org/abs/2502.17883>

Contini, M., Illien, V., Julien, M., Ravitchandirane, M., Russias, V., Lazennec, A., Chevrier, T., Rintz, C.L., Carpentier, L., Gogendeau, P., Leblanc, C., Bernard, S., Boyer, A., Daudon, J.T., Poulain, S., Barde, J., Joly, A., Bonhommeau, S., 2025b. Seatizen atlas: a collaborative dataset of underwater and aerial marine imagery. *Sci. Data* 12, 67. <https://doi.org/10.1038/s41597-024-04267-z>

Dodge, K.L., Kukulya, A.L., Burke, E., Baumgartner, M.F., 2018. Turtlecam: a “smart” autonomous underwater vehicle for investigating behaviors and habitats of sea turtles. *Front. Mar. Sci.* 5. <https://doi.org/10.3389/fmars.2018.00090>

Drap, P., 2012. Underwater photogrammetry for archaeology. In: Silva, D. C.d. (Ed.), *Special Applications of Photogrammetry*. IntechOpen, Rijeka. chapter 6. <https://doi.org/10.5772/33999>

Ferrari, R., 2017. 3D photogrammetry quantifies growth and external erosion of individual coral colonies and skeletons. *Sci. Rep.* 7 (1), 16737. <https://doi.org/10.1038/s41598-017-16408-z>

Gogendeau, P., Bonhommeau, S., Fourati, H., De Oliveira, D., Taillandier, V., Goharzadeh, A., Bernard, S., 2022. Dead-reckoning configurations analysis for marine turtle context in a controlled environment. *IEEE Sens. J.* 22 (12), 12298–12306. <https://doi.org/10.1109/JSEN.2022.3170414>

Gunner, R.M., 2021. Dead-reckoning animal movements in r: a reappraisal using gundog.tracks. *Anim. Biotelem.* 9 (1), 23. <https://doi.org/10.1186/s40317-021-00245-z>

Hodges, B.A., Grare, L., Greenwood, B., Matsuyoshi, K., Pizzo, N., Statom, N.M., Farrar, J.T., Lenain, L., 2023. Evaluation of ocean currents observed from autonomous surface vehicles section. *J. Atmos. Ocean. Technol.* <https://doi.org/10.1175/JTECH-D-23-0066.1>

Hyun, J.-H., Lee, D.-H., Jae-Cheol, L., 2023. Bathymetric surveying using autonomous surface vehicle for shallow-water area with exposed and partially exposed rocks. *Sens. Mater.* 35 (9), 3451. <https://doi.org/10.18494/SAM4478>

Iwata, T., Akamatsu, T., 2025. Blogging as a potential platform for resolving ocean environmental issues and threats: towards the development of the internet of animals. *Water Biol. Secur.*, 100383. <https://doi.org/10.1016/j.watbs.2025.100383>

Johnson-Roberson, M., Pizarro, O., Williams, S.B., Mahon, I., 2010. Generation and visualization of large-scale three-dimensional reconstructions from underwater robotic surveys. *J. Field Robot.* 27 (1), 21–51. <https://doi.org/10.1002/rob.20324>

Joseph, P., 1968. Applications of underwater photogrammetry. <https://apps.dtic.mil/sti/citations/AD0851692>

Kimball, P., et al., 2014. The WHOI jetyak: an autonomous surface vehicle for oceanographic research in shallow or dangerous waters. In: 2014 IEEE/OES Autonomous Underwater Vehicles (AUV), pp. 1–7. <https://doi.org/10.1109/AUV.2014.7054430>

Lambert, R., Page, B., Chavez, J., Mahmoudian, N., 2020. A low-cost autonomous surface vehicle for multi-vehicle operations. In: *Global Oceans 2020: Singapore – U.S. Gulf Coast*, pp. 1–5. <https://doi.org/10.1109/IEEECONF38699.2020.9389236>

Lavy, A., et al., 2015. A quick, easy and non-intrusive method for underwater volume and surface area evaluation of benthic organisms by 3D computer modelling. *Methods Ecol. Evol.* 6 (5), 521–531. <https://doi.org/10.1111/2041-210X.12331>

Liu, Z., Zhang, Y., Yu, X., Yuan, C., 2016. Unmanned surface vehicles: an overview of developments and challenges. *Annu. Rev. Control* 41. <https://doi.org/10.1016/j.arcontrol.2016.04.018>

Liu, Y., Xue, J., Wang, W., 2024. A high-precision, ultra-short baseline positioning method for full sea depth. *J. Mar. Sci. Eng.* 12 (10), 1689. Number: 10 Publisher: Multidisciplinary Digital Publishing Institute. <https://doi.org/10.3390/jmse12101689>

Marre, G., et al., 2019. Monitoring marine habitats with photogrammetry: a cost-effective, accurate, precise and high-resolution reconstruction method. *Front. Mar. Sci.* 6. <https://doi.org/10.3389/fmars.2019.00276>

Million, W.C., O'Donnell, S., Bartels, E., Kenkel, C.D., 2021. Colony-level 3D photogrammetry reveals that total linear extension and initial growth do not scale with complex

- morphological growth in the branching coral, *acropora cervicornis*. *Front. Mar. Sci.* 8. <https://doi.org/10.3389/fmars.2021.646475>.
- OpenDroneMap Development Team, 2025. OpenDroneMap: Open source toolkit for aerial image processing. Consulté le 12 mars 2025. <https://www.opendronemap.org/webodm/>.
- Organization, I.H., 2020. IHO Standards for Hydrographic Surveys, Edition 6.0.0. <https://doi.org/10.25607/OBP-1354.2>
- Page, B.R., Lambert, R., Chavez-Galaviz, J., Mahmoudian, N., 2021. Underwater docking approach and homing to enable persistent operation. *Front. Robot. AI* 8. <https://doi.org/10.3389/frobt.2021.621755>
- Raber, G.T., Schill, S.R., 2019. A low-cost small unmanned surface vehicle (sUSV) for very high-resolution mapping and monitoring of shallow marine habitats. In: *Remote Sensing of the Ocean, Sea Ice, Coastal Waters, and Large Water Regions 2019*. Bostater Jr., C.R., Neyt, X., Viallefont-Robinet, F. (Eds.), SPIE, p. 1115004. <https://doi.org/10.1117/12.2531361>
- Shiple, O.N., Nicoll, A., Cerrato, R.M., Dunton, K.J., Peterson, B.J., Sclafani, M., Bangley, C., Balazik, M.T., Breece, M., Cahill, B.V., Fox, D.A., Gahagan, B.I., Kneebone, J., Leone, F., Manz, M., Ogburn, M., Post, W.C., Scannell, B., Frisk, M.G., 2024. Performance of a fine-scale acoustic positioning system for monitoring temperate fish behavior in relation to offshore marine developments. *Anim. Biotelem.* 12 (1), 36. <https://doi.org/10.1186/s40317-024-00386-x>
- Sotelo-Torres, F., Alvarez, L.V., Roberts, R.C., 2023. An unmanned surface vehicle (USV): development of an autonomous boat with a sensor integration system for bathymetric surveys. *Sensors* 23 (9), 4420. Number: 9 Publisher: Multidisciplinary Digital Publishing Institute. <https://www.mdpi.com/1424-8220/23/9/4420>. <https://doi.org/10.3390/s23094420>
- Vlachos, M., et al., 2019. Software comparison for underwater archaeological photogrammetric applications. *Int. Arch. Photogramm., Remote Sens. Spat. Inf. Sci.* XLII-2/W15, 1195–1201. <https://doi.org/10.5194/isprs-archives-XLII-2-W15-1195-2019>
- Wardoyo, A., Sary, I., Maulana, I., 2022. An analysis of the performance of autonomous navigation on an ardupilot-controlled rover. *Ultima Comput.* 14, 82–87. <https://doi.org/10.31937/sk.v14i2.2844>
- Yan, R.-j., Pang, S., Sun, H.-b., Pang, Y.-j., 2010. Development and missions of unmanned surface vehicle. *J. Mar. Sci. Appl.* 9, 451–457. <https://doi.org/10.1007/s11804-010-1033-2>
- Zhao, Y., He, Z., Li, G., Wang, Y., Li, Z., 2020. Design and application of a small ROV control system based on ArduSub system. In: *2020 IEEE 2nd International Conference on Civil Aviation Safety and Information Technology (ICCSIT)*, pp. 585–589. <https://doi.org/10.1109/ICCSIT50869.2020.9368667>



Pierre Gogendeau completed his Ph.D. in Automatic Systems and Micro-electronics at the University of Montpellier in 2022 His Ph.D. thesis focused on developing a solution for underwater trajectory estimation and transmission that can be embedded within a bio-telemeter. Pierre holds a Master's degree in Electronics and Computer Engineering from INSA de Rennes, which he obtained in 2017. In the same year, he joined IFREMER to work on a research project as a marine instrumentation engineer, focusing on designing innovative and open-source devices for observing marine wildlife and its environment.



Sylvain Bonhommeau is a researcher in marine ecology at Ifremer in Reunion Island. His research focuses mainly focuses on oceanography, early life stages of marine species, fish migration, and tropical ecosystem biodiversity. He develops multidisciplinary approaches to improve scientific knowledge for a sound management of marine species.



Hassen Fourati, Ph.D., is currently an associate professor of the electrical engineering and computer science at the University of Grenoble Alpes, Grenoble, France, and a member of the Dynamics and Control of Networks Team (DANCE), affiliated to the Pôle Automatique et Diagnostic (PAD) of the GIPSA-Lab. He earned his bachelor of engineering degree in electrical engineering at the National Engineering School of Sfax (ENIS), Tunisia; master's degree in automated systems and control at the University of Claude Bernard (UCBL), Lyon, France; and Ph.D. degree in automatic control at the University of Strasbourg, France, in 2006, 2007, and 2010, respectively. His research interests include nonlinear filtering, estimation and multisensor fusion with applications in

navigation, motion analysis, mobility and traffic management. He has published several research papers in scientific journals, international conferences, book chapters and books. He can be reached at hassen.fourati@gipsa-lab.fr.



Mohan Julien holds a Master's degree in Electrical Engineering from INSA de Lyon, with a specialization in Embedded and Integrated Systems, obtained in 2014. In 2018, Mohan completed a Ph.D. in Microelectronics at the University of Montpellier, focusing on the CMOS design of high-performance integrated current sources for biomedical applications. Since 2019, he has been engaged in research projects with CNRS and IFREMER as a post-doctoral researcher and research engineer. His current research interests lie in the design of innovative and open-source devices for the observation of marine wildlife and its environment. This work encompasses CMOS design, the development and programming of embedded systems, the implementation of data collection networks, and the analysis of the collected data.



Matteo Contini received a M.Sc. degree in Mathematical Engineering at Politecnico di Milano with a double degree at Ecole Centrale de Lyon. He is currently a second year Ph.D. student at Ifremer in La Réunion. His current research focuses on the development of computer vision based algorithms on different scales for tropical reefs monitoring.



Thomas Chevrier is a Ph.D. student at the company COOOL in Reunion Island working on fish genetics and epigenetics. He completed a master in marine science in Brest on species and habitat identification using artificial intelligence.



Anne Elise Nieblas received the B. Science in marine biology and a B. Arts in Environmental Studies from the University of California, Los Angeles, USA in 2004, a B. Sciences (Honors, First Class) from the University of Tasmania (UTAS), Hobart, Australia in 2005, and a Ph.D. degree in Quantitative Marine Science (QMS) from the joint QMS program of UTAS and the Commonwealth Scientific Industrial Research Organisation, Hobart, Australia in 2010. She is now the president of the Company for Open Ocean Observations and Logging, Saint Leu, La Reunion, France. Her research interests focus on developing innovative tools and techniques to support a sustainable blue economy.



Serge Bernard received the Ph.D. degree in Electrical Engineering from the University of Montpellier, France in 2001. He is a researcher of the National Council of Scientific Research (CNRS) in the Microelectronics Department of the Laboratory of Computer Science, Robotics and Microelectronics of Montpellier (LIRMM). He was the director of the joint Institute for System Testing ISyTest between the LIRMM and NXP semiconductors. He was also the head of the microelectronics department of LIRMM. His main research interests include development of new tools for Ocean Observation and sensors for medical and environment applications. He has participated in the supervision of 22 Ph.D. dissertations, contributed to 3 patents, authored or co-authored over 120 international papers, and contributed to the redaction of 2 books on these topics.